Waste Management 165 (2023) 70–81

Contents lists available at ScienceDirect

Waste Management

journal homepage: www.elsevier.com/locate/wasman

Biorefining of rapeseed meal: A new and sustainable strategy for improving Cr(VI) biosorption on residual wastes from agricultural byproducts after phenolic extraction

Pei Liu [a,b,1], Yangmin Gong [a,b,1], Chen Yang [a,b], Rodrigo Ledesma-Amaro [c], Young-Kyoung Park [c], Shiyu Deng [a,b], Yuliang Wang [d], Hongbo Wei [e], Wenchao Chen [a,b,*]

[a] Oil Crops Research Institute of the Chinese Academy of Agricultural Sciences, Wuhan 430062, PR China
[b] Key Laboratory of Biology and Genetic Improvement of Oil Crops, Ministry of Agriculture, Wuhan 430062, PR China
[c] Department of Bioengineering and Imperial College Centre for Synthetic Biology, Imperial College London, London SW7 2AZ, UK
[d] Hubei University of Technology, Wuhan 430068, PR China
[e] Yangtze University, Jingzhou 434025, PR China

ARTICLE INFO

Keywords:
Rapeseed byproducts
Phenolic extract
Residual waste
Cr(VI) biosorption
Conjugational or free form of phenolics

ABSTRACT

Phenolic recovery from agricultural byproducts has been highlighted due to their health-promoting bioactivities. However, uncontrolled discard of residues after extraction process would induce environmental pollution and bioresource waste. In this study, biorefining of phenolic-rich rapeseed meal (RSM) and its defatted sample (dRSM) was attempted by holistic utilization of phenolic extract and residue separately. Phenolic removal could significantly improve residues' Cr(VI) adsorption capacities by about 21%, which presented extended physical surface and more released functional groups. Moreover, simulating raw material by remixing 3% separated phenolic extracts or main component sinapic acid therein with corresponding residues further improved about 12% adsorption efficiencies. These indicated that the different present forms of phenolics had opposite effects on Cr(VI) removal. While natural conjugational form inhibited hosts' biosorption, free form had enhanced functions for either extract or residue. Four optimal adsorption parameters (pH, adsorbent dosage, contact time and initial Cr(VI) concentration), three kinetic (pseudo-first order, pseudo-second order and intra-particle diffusion) models and two isotherms (Langmuir and Freundlich) were used to reveal the adsorption process. The maximum Cr(VI) adsorption capacity on residues could reach about 100 mg/g, which was superior to that of most biosorbents derived from agricultural byproducts, even some biochar. Together with the residues' advantages with everlasting capacity after 3 adsorption–desorption cycles and excellent abilities for adsorbing multiple co-existed metal ions (Cr(VI), Cd(II), Cu(II), Pb(II), Ni(II) and Zn(II)), phenolic recovery was first proved to be a new and sustainable strategy for modifying biosorbents from agricultural byproducts with zero waste.

1. Introduction

Rapeseed is the second most widely produced oil crops in the world (Hu et al., 2022). Rapeseed meal (RSM), as its dominant byproduct after oil extraction, mainly composes of protein, lignin, cellulose and hemicellulose (Di Lena et al., 2021; Morosanu et al., 2019), which is similar to the major constituents of lignocellulose (Ravindran and Jaiswal, 2016). Due to the abundant content of phenolic compounds, rapeseed byproducts have been widely used as raw materials for extraction. These phenolic extracts from rapeseed byproducts possess a variety of functions, mainly due to their antioxidant and antimicrobial bioactivities, including (i) relieving oxidation of cellular molecules such as DNA, lipids and proteins (Pohl et al., 2018), (ii) improving microbial and oxidative stability of nutritional ingredients (Kim and Lee, 2017), and (iii) hepatoprotective, neuroprotective, anti-obesity, anticarcinogenic and antimutagenic properties (Hussain et al., 2019; Li and Guo, 2016; Nandasiri et al., 2019; Quinn et al., 2017; Yates et al., 2019). However, a largely overlooked challenge associated with phenolic recovery from agricultural byproducts is how to deal with the residual wastes after extraction process. Uncontrolled discard of these residues would not

* Corresponding author at: Oil Crops Research Institute of the Chinese Academy of Agricultural Sciences, Wuhan 430062, PR China.
E-mail address: chenwenchao01@caas.cn (W. Chen).
[1] P. Liu and Y. Gong contributed equally to this work.

https://doi.org/10.1016/j.wasman.2023.04.024
Received 10 February 2023; Received in revised form 2 April 2023; Accepted 12 April 2023
Available online 20 April 2023
0956-053X/© 2023 The Author(s). Published by Elsevier Ltd. This is an open access article under the CC BY-NC-ND license (http://creativecommons.org/licenses/by-nc-nd/4.0/).

only induce environmental pollution but also cause bioresource waste.

It has been reported that rapeseed waste could be reused for sequential biosorption of lead (II) and Rb19 dye pollutants (Morosanu et al., 2019). Moreover, biochar produced by pyrolysis of rapeseed cake was characterized with a high affinity for copper (II) and zinc (II) and a relatively low affinity for arsenic (III) (Mazurek et al., 2021), suggesting that rapeseed byproducts have the potential to remove many heavy metal ion pollutants. Hexavalent chromium (Cr(VI)), mainly discharged from industries working on electroplating, smelting, dyeing, leather, battery manufacturing, mining operations and chemical manufacturing (Dong et al., 2021; Mallik et al., 2022; Qiu et al., 2020; Suksabye and Thiravetyan, 2012), is classified as the number one carcinogenic, teratogenic and mutagenic agent (Orooji et al., 2021). Its toxicity can cause lung cancer and other human diseases including damage to brain, liver and kidney (Chen et al., 2019; Nahar et al., 2018). Therefore, it is necessary to remove Cr(VI) from wastewater stream before being released into the environment. However, whether RSM and its residue after extraction process are able to directly adsorb Cr(VI) is still an open question.

Another point worth considering is whether phenolic removal would affect the adsorption properties of RSM. Phenolics, which are considered as major plant secondary metabolites, are much richer in rapeseed than in other oil crop seeds (He et al., 2022). Because of most phenolics remaining in byproducts after oil extraction, their interactions with proteins not only result in unpleasant color, bitter taste and poor digestibility, but also diminish antioxidant capacity (Alu'datt et al., 2017; Hernández-Jabalera et al., 2015; Zhu et al., 2018). Our previous study demonstrated that phenolic compounds in RSM could hamper protein feedstock for the microbial production of iturin A (Wang et al., 2021). Moreover, covalent and non–covalent interactions between phenolics and polysaccharides exert great impacts on each accessibility and bioactivity (Alu'datt et al., 2017; Hernández-Jabalera et al., 2015; Zhu et al., 2018). However, there is still no report about the effect of phenolics on other characteristics of rapeseed byproducts, including heavy metal adsorption.

There are two opposite opinions about the function of phenolics in RSM regarding Cr(VI) adsorption. (i) The phenolic groups in green waste with high phenolic content have positive effects on heavy metal ion adsorption. After adsorbed, Cr(VI) can be then reduced and detoxified to Cr(III) through the phenolic aromatic ring which acts as an electron donor (Kuppusamy et al., 2015). Therefore, if phenolics in RSM are extracted, the adsorption capacity of residues would be reduced. (ii) In natural agricultural byproducts, mutual interactions between phenolics and other components always inhibit each function: the conjugational forms not only suppress phenolics' functional activity, but also restrain the porous structure, specific surface area and surface active chelating sites of other components (Alu'datt et al., 2017; Hernández-Jabalera et al., 2015; Zhu et al., 2018). From this point of view, phenolic removal from RSM might be a feasible strategy to improve the adsorption capacity of residues.

In this study, from RSM and its defatted sample (dRSM), two phenolic extracts (RSM-E and dRSM-E) and two residues (RSM-R and dRSM-R) were produced. To understand how Cr(VI) adsorption is affected by phenolics in agricultural byproducts, the removal performances of Cr(VI) with different raw materials and corresponding residues were comparatively analyzed. Their surface morphology and structural characteristics were identified by SEM and FTIR. Moreover, individual and combined influences of phenolic extract and residue were also explored to shed light on the role of phenolics with either conjugational or free form during Cr(VI) removal process. Because the phenolic extracts can be used to exploit innovative functional products for the cosmetic, food, feed, pharmaceutical and nutraceutical sectors (Hussain et al., 2019; Kim and Lee, 2017; Li and Guo, 2016; Nandasiri et al., 2019; Pohl et al., 2018; Quinn et al., 2017; Yates et al., 2019), and therefore contribute towards the development of zero waste biorefinery, we also investigated the optimal conditions, the adsorption kinetics and isotherms for Cr(VI) adsorption with residues, respectively. In order to further expand the application value of biosorbents derived from rapeseed byproducts, the regenerability and the adsorption affinity for other heavy metal ions besides Cr(VI) were also assessed.

2. Materials and methods

2.1. Materials and chemicals

RSM used in the experiments were kindly supplied by the Oil Crops Research Institute (OCRI) of the Chinese Academy of Agricultural Sciences (CAAS) (Wuhan, China), then dried at 60 °C to constant weight, and grounded through 40 mesh sieve. Then partial RSM was defatted with hexane in a solid–liquid ratio of 1:3 (w/v, g/mL) at room temperature. After ultrasound for 40 min, precipitations were collected by filtration with gauze. The above steps were repeated three times. To remove the residual hexane, extracted samples were air-dried overnight in the laboratory hood. The final defatted material from RSM was designated as dRSM. Chemicals such as $K_2Cr_2O_7$, $NiCl_2$, $CuCl_2$, $ZnCl_2$, $CdCl_2$, and $PbCl_2$ were of analytical grade (Sinopharm Group Chemical Reagent Co. Ltd, Shanghai, China). Sinapic acid (SA) and melanin (ME) was purchased from Sigma (Germany).

2.2. Phenolic extraction and residue production

Phenolics were extracted according to a reported method (Wang et al., 2021) with some modifications. In this study, RSM and dRSM were mixed with 54% ethanol solution containing 1 mol/L HCl at a ratio of 1:10 (w/v). The mixture was shaken at 150 rpm at 55 °C for 1.5 h, followed by centrifugation at 4000 rpm for 20 min. The obtained supernatant was poured on an AB-8 macroporous resin (HaoJu resin Technology Co. Ltd., Tianjin, China) and then eluted with a standard 70% ethanol solution. The ethanolic fractions were dried with a vacuum evaporator and the phenolic extracts derived from RSM and dRSM were designated as RSM-E and dRSM-E, respectively. Moreover, the corresponding residues were dried in the oven at 60 °C and designated as RSM-R and dRSM-R, respectively.

2.3. Characterization

Fourier transform infrared (FTIR) spectra were detected on a TENSOR 27 spectrophotometer (BRUKER, Germany)) using KBr pellets in the range from 4000 to 400 cm^{-1} under a resolution of 2 cm^{-1} at ambient temperature (Di Lena et al., 2021; Feng et al., 2021). The surface morphology of all adsorbents was characterized by a Scanning Electron Microscope (HITACHI U8010, HITACHI, Japan). The total phenolic content was determined using the Folin−Ciocalteu assay, according to the method described previously by Quinn et al. (2017).

2.4. Adsorption experiments

Adsorption experiments were conducted in a series of 125 mL conical flasks with 30 mL Cr(VI) solution. These conical flasks were incubated at room temperature in a constant temperature shaker at 150 rpm. Unless otherwise noted, the usual adsorption conditions were pH 2.0, 0.15 g/ 30 mL adsorbent dosage, 300 min contact time and 100 mg/L initial Cr (VI) concentration. Effects of key parameters including pH (2.0, 3.0, 4.0, 5.0, 6.0, 7.0), adsorbent dosage (0.05, 0.10, 0.15, 0.20, 0.25, 0.30 g/ 30 mL), contact time (30, 60, 120, 180, 240, 300, 360, 420, 480 min) and initial Cr(VI) concentration (100 to 1000 mg/L) were systematically investigated. The Cr(VI) concentrations were quantified using a 1,5-diphenylcarbazide colorimetric method (Dong et al., 2021). All adsorption experiments were operated at least in triplicate.

2.5. Adsorption kinetic studies

Based on the relationship between contact time and adsorption capacity (q_e), the kinetics of adsorption of Cr(VI) was described by the pseudo-first order, pseudo-second order and intra-particle diffusion models (Balasubramanian et al., 2020; Chen et al., 2021; Quyen et al., 2021).

The equation of the pseudo-first order kinetic model is given by:

$$\ln(q_e - q_t) = \ln q_e - k_1 t \quad (1)$$

where q_e is the adsorption capacity of the metal ion at the equilibrium (mg/g), q_t is the adsorption capacity of the metal ion at t time, k_1 is the rate constant of the pseudo-first order kinetic model (min^{-1}).

The pseudo-second order kinetic equation can be written as follows:

$$\frac{t}{q_t} = \frac{1}{k_2 q_e^2} + \frac{t}{q_e} \quad (2)$$

where k_2 is the rate constant of the pseudo-second order kinetic model (g• mg^{-1}• min^{-1}).

The intra-particle diffusion equation is as follows:

$$q_t = k_3 t^{0.5} + C \quad (3)$$

where k_3 is the rate constant of intra-particle diffuse model (mg• g^{-1}• $min^{-0.5}$), C is associated to the boundary layer thickness.

2.6. Adsorption isotherms

The relationship between the initial metal concentration and the capacity of adsorbent can be described by the adsorption isotherm. In this paper, the adsorption isotherm models of Langmuir and Freundlich were used to evaluate the equilibrium data (Balasubramanian et al., 2020; Chen et al., 2021; Quyen et al., 2021).

Langmuir isotherm model is as follows:

$$q_e = \frac{q_m k_L C_e}{1 + k_L C_e} \quad (4)$$

where q_e is the adsorption capacity of the metal ion at the equilibrium (mg/g), q_m is the monolayer sorption capacity of the adsorbent (mg/g), C_e is the equilibrium Cr(VI) concentration in the solution (mg/L), k_L is the constant of Langmuir (L/mg).

Freundlich isotherm model can be written as follows:

$$q_e = k_F C_e^{1/n} \quad (5)$$

where k_F is Freundlich constant ((mg• g^{-1})(mg• L^{-1})$^{-n}$), n is adsorption intensity.

2.7. Regeneration test

The adsorbents after adsorbing Cr(VI) were desorbed with 0.1 M NaOH solution. Referring to the method described by Shan et al. (2020), the specific operation was as follows: 0.15 g of adsorbents after adsorbing Cr(VI) were placed in 30 mL of 0.1 M NaOH solution, and shaken at 150 rpm for 3 h at room temperature. The desorbed adsorbents were dried after being washed with deionized water to neutrality, and then used for the regeneration experiment with 100 mg/L Cr(VI) solution. The above steps were repeated until four adsorption–desorption cycles were completed.

2.8. Effect of co-existing ions on adsorption

A cationic pollution system is prepared from $K_2Cr_2O_7$, $NiCl_2$, $CuCl_2$, $ZnCl_2$, $CdCl_2$ and $PbCl_2$ so that the initial concentrations of Cr(VI), Ni(II), Cu(II), Zn(II), Cd(II) and Pb(II) ions were 100 mg/L. The other adsorption conditions were pH 2.0, 0.15 g/ 30 mL adsorbent dosage and 300 min contact time. Amounts of Cr(VI), Ni(II), Cu(II), Zn(II), Cd(II) and Pb(II) ions in the solution after the adsorption reaction were measured using ICP-OES (ICAP PRO, Thermo Fisher, USA).

3. Results and discussion

3.1. Improvement of Cr(VI) adsorption on rapeseed byproducts by phenolic extraction

Whether defatted or not, RSM and dRSM showed strong adsorption capacity for Cr(VI), which has not yet been reported in the literature. When the adsorbent dosage was 0.05 g/ 30 mL, the Cr(VI) adsorption amounts reached 30.36 and 30.13 mg/g with RSM and dRSM, and the corresponding efficiencies were 50.60% and 50.22%, respectively. An interesting phenomenon was that the phenolic extraction process could increase Cr(VI) adsorption on residues. Compared with the original materials, the Cr(VI) removal efficiencies were increased by 1.22– and 1.19-fold with RSM-R and dRSM-R, respectively (Fig. 1). Although the defatted process did not improve the adsorption affinity for Cr(VI), the phenolic extraction might be regarded as a general and effective strategy to modify the Cr(VI) adsorption of phenolic-rich agricultural byproducts. This new modification accompanied phenolic recovery is consistent with the concept of biorefinery. Compared with other modification, such as pyrolysis or chemical modification, this strategy possesses advantages including low-cost and zero-waste, which can create a new direction for the integrated valorization of rapeseed byproducts with simultaneous recovery of phenolics and improvement of residues' Cr(VI) adsorption.

3.2. Characterization of biosorbents derived by phenolic extraction

In order to compare the surface morphology of the biosorbents before and after phenolic extraction, Scanning Electron Micrograph (SEM) analysis was performed on two raw materials (RSM and dRSM) and two residues (RSM-R and dRSM-R). As shown in Fig. 2A-2D, a common structural feature of RSM and its derivatives was a stable honeycomb porous skeleton, which was not destroyed by either the defatted or the phenolic extraction process. However, the pores were filled with components such as proteins, fats and phenolics so that the surface of RSM was basically free of pores. Fats can increase the non-covalent adhesion of different components, while phenolics can interact covalently or non-covalently with other components including peptides and polysaccharides (Alu'datt et al., 2017; Hernández-Jabalera et al., 2015; Zhu et al., 2018). Therefore, individual process of defatted or phenolic extraction could expose some pores. The main difference

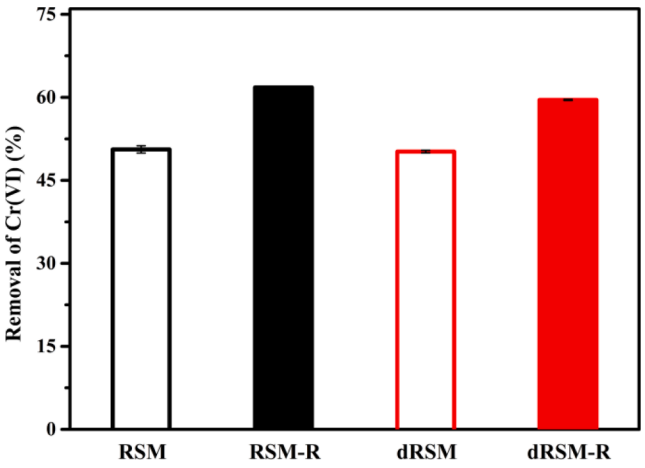


Fig. 1. Effect of phenolic extraction from rapeseed byproducts on Cr(VI) removal efficiencies.

was that the former could make the cleaner and smoother surface of the honeycomb porous structure with smaller pore size, while the latter resulted in a looser structure with many particles adhered on the surface (both inside and outside the pores). Furthermore, the combination of both methods resulted in the clean exposure of nearly all pores.

Comparing the results from Fig. 1 and Fig. 2A-2D, we concluded that the highly porous structure produced by the defatted process had no significant influence on improving the Cr(VI) adsorption capacity of corresponding samples (dRSM vs RSM, dRSM-R vs RSM-R). However, it has been reported that the increase in porosity could enhance the contact area between adsorbent and heavy metals, which was beneficial to adsorption (Mallik et al., 2022). Therefore, we speculated that the defatted process might simultaneously cause another detrimental effect on Cr(VI) adsorption, which offset the above benefit. The most likely

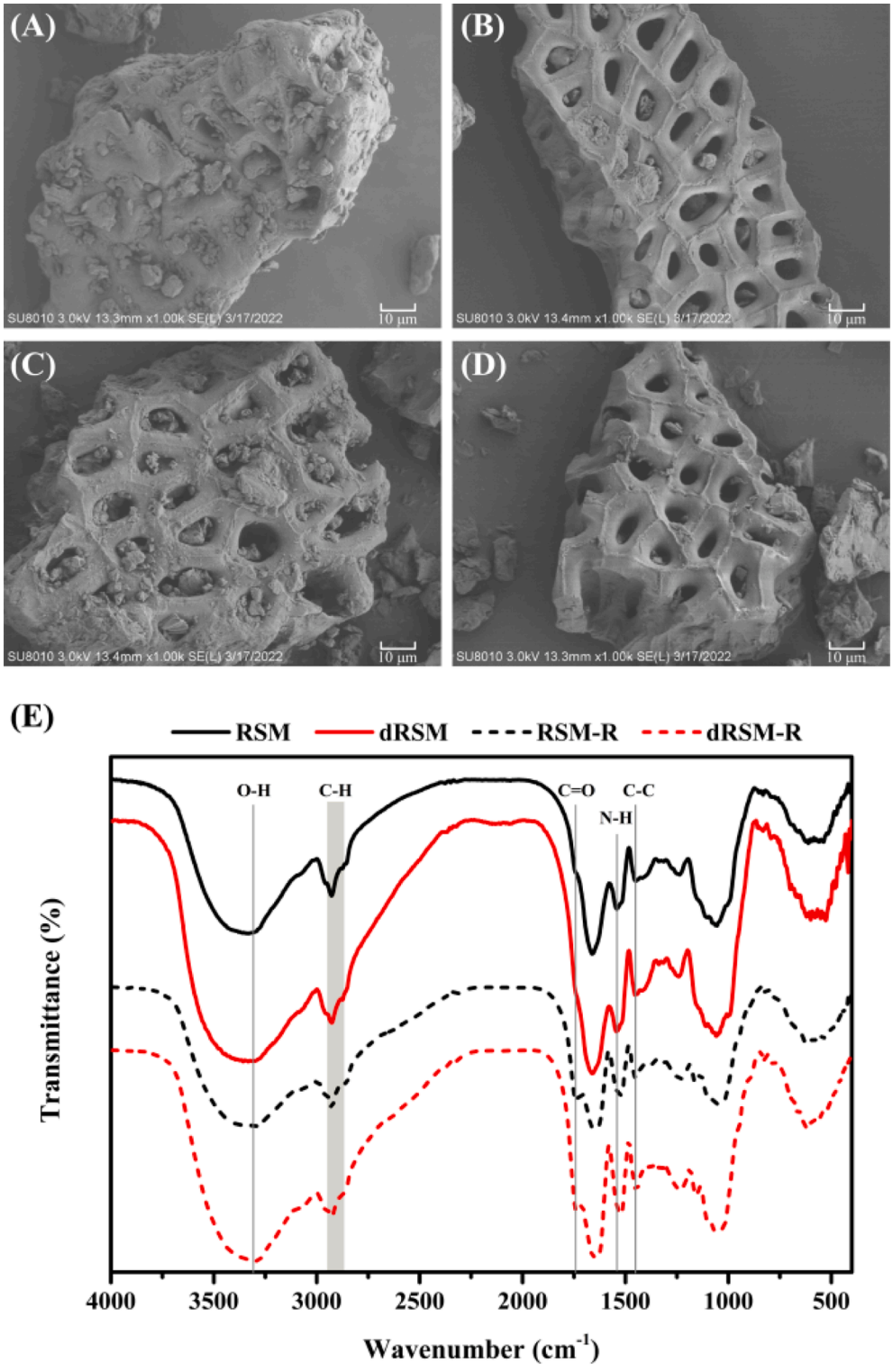


Fig. 2. Characterization of biosorbents derived by phenolic extraction. SEM image of RSM (A), dRSM (B), RSM-R (C) and dRSM-R (D); (E) FTIR spectra of RSM, dRSM, RSM-R and dRSM-R.

reason is that particles with adsorption-promoting groups (especially N-containing functional groups) (Chen et al., 2021; Leng et al., 2020; Mazurek et al., 2021; Mallik et al., 2022; Zhao et al., 2021), adhered on skeleton surface, were eluted by the defatted process. In addition, phenolic extraction could greatly improve residues' affinity for Cr(VI), which might be mainly caused by the release of adsorption-promoting functional groups shielded by phenolics with the conjugational form rather than a physical change in structure (Alu'datt et al., 2017; Hernández-Jabalera et al., 2015; Zhu et al., 2018). Although this cannot be demonstrated in the experimental results of SEM, it is consistent with the report by Zhang et al. (2019), and suggests that the surface adsorption-promoting groups play a more crucial role than the pore morphology in the heavy metals adsorption.

In order to investigate the possible adsorption mechanism of RSM and its derivatives for Cr(VI), FTIR analysis was performed (Fig. 2E). The wider peak at around 3300 cm^{-1} accords with the O–H bonds, which can be ascribed to the polysaccharides, cellulose (Di Lena et al., 2021) and/or phenolics (Thakur and Nanda, 2019). Symmetric and asymmetric stretching modes of CH_2 are found at 2855 cm^{-1} and 2925 cm^{-1}, which are mainly attributed to the hydrocarbon chains such as those of fatty

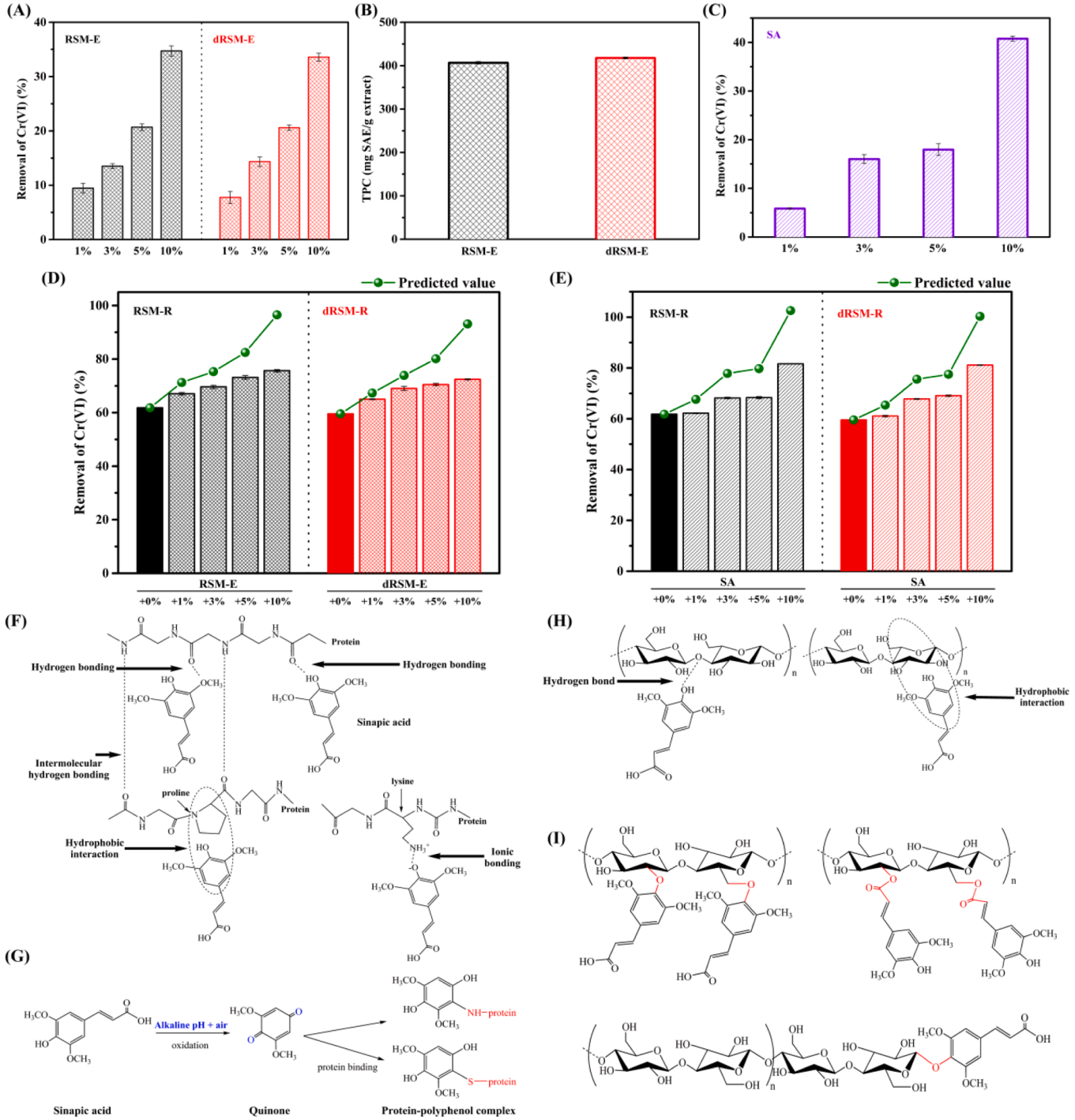


Fig. 3. Influences of phenolics with the free form on Cr(VI) adsorption capacity. (A) Cr(VI) adsorption capacity and (B) TPC of different phenolic extracts; (C) Cr(VI) adsorption capacity of SA; Combinations of different concentrations of phenolic extracts (D) or SA (E) with corresponding residues; (F) Non-covalent and (G) covalent interaction between protein and SA; (H) Non-covalent and (I) covalent interaction between cellulose and SA.

acids (Filipowiak et al., 2021), whose peak intensity would decrease through the defatted process. A new peak at 1739 cm^{-1} is associated with the phenolic extraction process and corresponds to the C=O stretching of the ester groups presented in the pectins, lignin, fatty acids and their glyceride derivatives. The peak intensity of the N–H groups greatly increases and shifts from 1543 cm^{-1} to 1522 cm^{-1} (RSM-R and dRSM-R) due to the phenolic extraction process. Although the region from 1500 cm^{-1} to 1000 cm^{-1} is informative, it is hard to analyze due to its complexity. Therein, the aromatic C–C bond at 1413 cm^{-1} is associated with phenolics.

3.3. Influences of phenolics with the free form on Cr(VI) adsorption capacity

Naturally extracted phenolics have been recognized as an effective and potential material in wastewater treatment by chelating and reducing various heavy metal ions (Kuppusamy et al., 2015). However, phenolics existed in rapeseed byproducts and their derivatives seemed to hinder Cr(VI) adsorption rather than promoting it in this study. In order to understand the causes of this phenomenon, the role of phenolic extracts on Cr(VI) adsorption was determined. As shown in Fig. 3A, both phenolic extracts (RSM-E and dRSM-E) possessed the ability to adsorb Cr (VI) with positive concentration dependence. This similar trend was correlated with the total phenolic contents (TPC) in both extracts (Fig. 3B).

Besides TPC, the specific profile of the phenolic extract might be another key factor to alter Cr(VI) adsorption capacity, which was previously reported to influence their antioxidant properties (Wang et al., 2021). Sinapic acid (SA) was a main component in phenolic extracts from rapeseed byproducts. Therefore, its Cr(VI) affinity was also measured. As shown in Fig. 3C, SA could remove Cr(VI) from water and the removal efficiency increased with the increase in concentration, which might be related to its antioxidant property to reduce Cr(VI) into Cr(III) (Kuppusamy et al., 2015).

With verification of the adsorption capacities of two phenolic extracts, another question arose: why did the original materials (RSM and dRSM) containing abundant phenolic content possess weaker Cr(VI) adsorption capacity than that of corresponding residues (RSM-R and dRSM-R) by phenolic removal? This seems to be a paradox that “one plus one is less than one”. Therefore, different concentrations of phenolic extracts or SA were remixed with their corresponding residues to simulate the natural composition of RSM or dRSM. Not surprisingly, as the concentration of added phenolic extracts or SA increased, the mixtures showed an increase in their Cr(VI) adsorption capacities (Fig. 3D and 3E). And more notably, the adsorption efficiencies were improved by about 12% when the additive amount was 3%, which was close to the extraction efficiency of phenolics. These indicated that the conjugational or free form of phenolics in the biosorbent played a crucial role in Cr(VI) adsorption capacity. In the original materials, the majority of phenolics existed in an conjugated form with other components, which mutually shielded the Cr(VI) adsorption functional groups of different components (Alu’datt et al., 2017; Hernández-Jabalera et al., 2015; Zhu et al., 2018). Through the extraction process, most phenolics were recovered to the free form, which could release the Cr(VI) adsorption capacity of both phenolics and residues. Although the Cr(VI) adsorption capacity of the corresponding mixture was greater than that of any single one (phenolic extract or residue), it was still less than the sum of these two. And the gap between the Cr(VI) removal efficiency of the corresponding mixture and the sum of these two would become bigger with the increased concentration of supplements. In other words, “one plus one is less than two”. This could be explained by partially separated phenolics re-bonded to the residue by the increased contact and reaction frequency with the increased concentration, which was consistent with the report described simultaneous adsorption of Cr(VI) and phenolics by biochar-based iron oxide composites in wastewater (Dong et al., 2021).

Taking SA as an example, the interaction mechanism of phenolics with proteins/cellulose, which were the major components in residues in this study, was shown in Fig. 3F-3I. The non-covalent interactions between SA and protein mainly included hydrophobic, electrostatic, hydrogen bond and inter-molecular interaction (Fig. 3F) (Le Bourvellec and Renard, 2010; Li et al., 2021). SA could also form quinones and covalently interact with proteins (Fig. 3G) (Yang et al., 2021). The non-covalent interactions between SA and cellulose mainly included hydrophobic interactions and hydrogen bonds (Fig. 3H), while they could be also covalently linked by ester, ether and glycosidic bonds under certain conditions (Fig. 3I) (Quíros-Sauceda et al., 2014). Taken together, all these results further indicated that the interaction between phenolics and components in the residue was an important factor affecting Cr(VI) adsorption capacity.

3.4. Effects of various adsorption parameters on different biosorbents

Cr(VI) elimination by adsorption is affected by various parameters such as pH, adsorbent dosage, contact time and initial Cr(VI) concentration. In this study, Cr(VI) removal efficiencies were determined under different conditions.

3.4.1. pH

Solution pH is important for the adsorption of different heavy metal ions. pH variation influences the diffusion, functional groups’ charge and linking properties of heavy metal ions on adsorbents (Zhang et al., 2018). At the same time, the specification of heavy metal ions would also be affected (Banerjee et al., 2018; Feng et al., 2021; Shi et al., 2020; Suksabye and Thiravetyan, 2012). In this study, the function of pH within the range of 2 to 7 on Cr(VI) adsorption capacity was explored (Fig. 4A). A commonly observed trend was that the Cr(VI) adsorption capacity of all biosorbents gradually decreased with the increase of pH. Taking dRSM-R as an example, its Cr(VI) removal efficiency decreased from 98.91% to 29.91%, when the pH value increased from 2 to 7. However, under any different pH condition, the residues had a high affinity for Cr(VI) compared to the original materials. Besides further proving the improvement of Cr(VI) adsorption by phenolics removal, pH 2 was chosen as an appropriate condition for followed experiments.

3.4.2. Adsorbent dosage

As expected, increasing the amount of adsorbents led to a larger surface area for adsorption, resulting in a higher removal efficiency (Fig. 4B). When the dosage was 0.30 g/ 30 mL, all removal efficiencies by these four biosorbents could reach higher than 99%. However, 0.15 g/ 30 mL might be a turning point, after which the increased rate of removal efficiency slowed down with the further increase of adsorbent dosage. Therefore, an adsorbent dosage of 0.15 g/ 30 mL was employed in subsequent experiments from the perspective of comprehensive cost. Similarly, the advantages of Cr(VI) adsorption caused by phenolic separation were also reflected in the optimizing dosage experiment.

3.4.3. Contact time

The results showed that the longer the contact time, the higher the removal efficiency (Fig. 4C). However, the Cr(VI) adsorption increased rapidly within the first 30 min. The removal efficiencies by RSM and dRSM reached 77.12% and 76.35% at 30 min, while phenolic extraction could further improve Cr(VI) removal efficiencies to 83.55% and 81.87% by corresponding residues (RSM-R and dRSM-R), respectively. The removal ratios gradually reached equilibrium values at 300 min, which enhanced to 95.06% by RSM and 94.75% by dRSM. Compared with two original materials, their corresponding residues further increased to higher than 98%. While the rapid first phase is reported to correspond to surface-bound adsorption of heavy metal ions, the slow second phase means the long-range diffusion into the adsorbent interior pores (Swarnalatha and Ayoob, 2016). In general, at any contact time, the residues were more effective than the materials before phenolic extraction at eliminating Cr(VI).

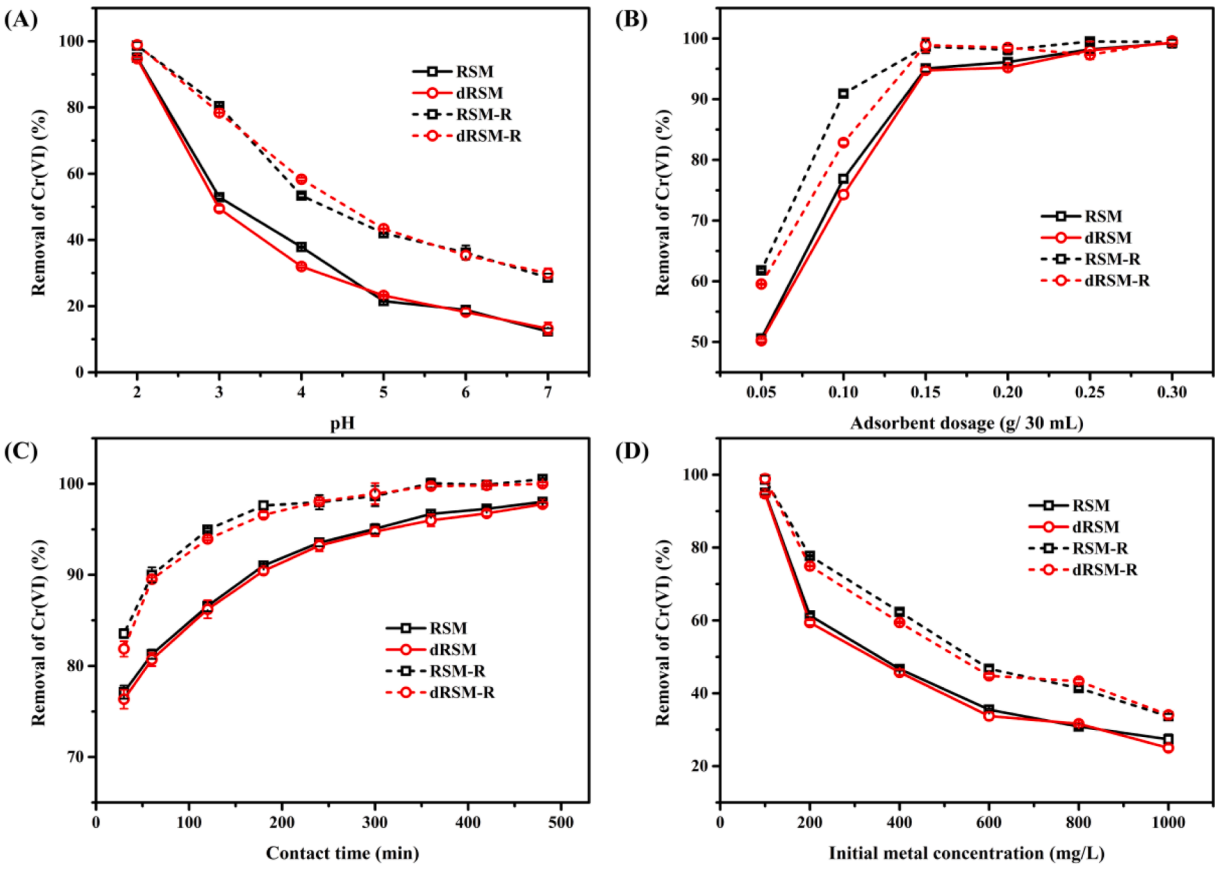


Fig. 4. Effects of various adsorption parameters on different biosorbents from rapeseed byproducts, including pH (A), adsorbent dosage (B), contact time (C) and initial Cr(VI) concentration (D).

3.4.4. *Initial Cr(VI) concentration*

Fig. 4D showed the influence of initial Cr(VI) concentration on removal efficiency. 0.15 g adsorbent and 30 mL solution were mixed well under pH 2 and samples were withdrawn at 300 min. The highest removal efficiency was achieved at a low initial Cr(VI) concentration, and it decreased as the concentration increased. At low concentration, Cr(VI) was adsorbed by specific adsorption sites. At higher concentrations of heay metal ions, the adsorption process slowed down due to adsorbent surface saturation, ultimately reaching an equilibrium state. The affinity for Cr(VI) followed the order: dRSM-R (34.03%) > RSM-R (33.71%) > RSM (27.35%) > dRSM (24.99%), when the initial Cr(VI) concentration reached 1000 mg/L.

3.5. *Adsorption kinetics*

Adsorption kinetics, which depends upon the mass transfer process as well as the physical and chemical properties of adsorbent, is a key for predicting an adsorption program. In this study, the kinetic data were examined by the pseudo-first order, pseudo-second order and intra-particle diffusion models. Fig. S1 show that the adsorption kinetics for Cr(VI) ions on RSM and their derivatives was best depicted by the pseudo-second-order model with higher correlation coefficients R^2 (>0.99) and closer specific adsorption amount to the actual experimental adsorption data. An interesting phenomenon was that R^2 of the pseudo-first-order and pseudo-second-order model on corresponding residues were slightly higher than that on two original materials (Table 1). On the contrary, R^2, which ranged from 0.96 to 0.83 on RSM and its derivatives, would be decreased on adsorbents modified by phenolic extraction, when the intra-particle diffusion model was employed. The lower value of R^2 for the intra-particle diffusion models indicated that the Cr(VI) adsorption was a multi-step procedure, including surface adsorption and interior diffusion (Halysh et al., 2018). These indicated that phenolic removal from RSM and dRSM could further expose the interior space for adsorption. Rather than intra-particle diffusion, the rate-limiting step was chemisorption through strong interaction and complexation between heavy metal ions and functional groups of adsorbents during the adsorption process (Balasubramanian et al., 2020; Quyen et al., 2021). However, the maximum

Table 1
Parameters in the three kinetic models for Cr(VI) adsorption on RSM and its derivatives.

Sample name	$q_{e,exp}$ (mg/g)	Pseudo-first-order			Pseudo-second-order			Intra-particle diffusion		
		$q_{e,cal}$ (mg/g)	k_1 (min^{-1})	R^2	$q_{e,cal}$ (mg/g)	k_2 ($g \cdot mg^{-1} \cdot min^{-1}$)	R^2	C	k_3 ($mg \cdot g^{-1} \cdot min^{-0.5}$)	R^2
RSM	19.60	18.68	0.0516	0.9750	19.54	0.0053	0.9933	14.37	0.2580	0.9578
dRSM	19.55	18.59	0.0507	0.9749	19.47	0.0052	0.9934	14.22	0.2612	0.9567
RSM-R	20.11	19.60	0.0598	0.9927	20.24	0.0074	0.9995	16.49	0.1840	0.8335
dRSM-R	20.00	19.54	0.0569	0.9923	20.22	0.0067	0.9995	16.17	0.1984	0.8327

adsorption capacities of residues were higher than that of original materials.

3.6. Adsorption isotherms

In order to build the most appropriate correlation between adsorbate and adsorbent for the equilibrium data, Langmuir and Freundlich isotherms were used to evaluate the adjustable parameters (Swarnalatha and Ayoob, 2016). While the Langmuir isotherm assumed a mono-layer adsorption at specific homogeneous sites on the surface, the Freundlich isotherm was suitable for multi-layer and heterogeneous surface adsorption (Suksabye and Thiravetyan, 2012). In this study, both Cr(VI) adsorption isotherms on biosorbents derived from RSM seemed to be fitted well with the experimental data, according to the coefficient correlations R^2, higher than 0.95 (Table 2). The applicability of these two isotherms suggested that both mono-layer and multi-layer adsorption were possible (Fig. S2). However, a comparison between these two isotherms demonstrated that the Freundlich model with higher R^2 values fitted better than Langmuir model. Moreover, the values of 1/n, ranged from 0.1 to 1.0 (Shan et al., 2020; Vázquez et al., 2009), suggested the favorable adsorption of Cr(VI) on the RSM and its derivatives surface. According to the Langmuir isotherm, the maximum adsorption capacities of Cr(VI) on RSM, dRSM, RSM-R and dRSM-R were 71.45, 66.53, 95.45 and 102.09 mg/g. Obviously, the biosorbents modified by phenolic extraction showed higher adsorption capacities, which were superior to that of most biosorbents derived from agricultural byproducts, even some biochar (Table S1).

3.7. Evaluation of the regeneration performance and the adsorption capacity for other heavy metals

The regeneration is one of the vital factors in assessing the adsorbent's potential for commercial applications in terms of saved cost and reduced environmental burden (Kekes et al., 2021). Since the Cr(VI) adsorptions on RSM and its derivants were favorable at acidic conditions, NaOH solution was selected as the desorption agent in this study. The Cr(VI) removal efficiencies on four biosorbents at the equilibrium form after each adsorption–desorption cycle were shown in Fig. 5A. The influence on the adsorption capacities of residues by the first, second and third cycle could almost be ignored. Because of the existence of a large number of reversible sites, both biosorbents exhibited satisfactory regeneration abilities and high reuse performances (Cherdchoo et al., 2019). For RSM and dRSM with relatively higher protein content, the gradual decreases of their adsorption capacities for Cr(VI) with the increase of cycle times might be contributed to the decreased amount of amine groups after the alkali desorption, which functioned as the electron donor for reducing Cr(VI) (Chen et al., 2021; Mazurek et al., 2021; Mallik et al., 2022; Zhao et al., 2021). However, no matter in which cycle, the residues after phenolic extraction showed greater adsorption capacities than the original materials. After four batches of adsorption–desorption cycles, each biosorbent still retained high adsorption efficiency exceeding 60%, which further declared the strong recyclability of RSM and its derivatives for Cr(VI) adsorption.

Compared with other biosorbents, dRSM-R possessed the best adsorption capacity and regenerability. Therefore, its adsorption characteristics needed to be more deeply studied. Since Ni(II), Cu(II), Zn(II), Cd(II) and Pb(II) were the most common co-existed ions in the heavy metal polluted soil and water (Rasool et al., 2022; Tauqeer et al., 2022; Turan et al., 2018a, 2018b), their effects on dRSM-R for Cr(VI) adsorption were investigated under polynary system. As shown in Fig. 5B, under the same concentration of all metal ions, dRSM-R had an obvious adsorption preference for Cr(VI). However, compared with the high adsorption efficiency of 98.91% by dRSM-R in a single system, its adsorption efficiency for Cr(VI) decreased to 76.92% in a polynary system. This might be associated with the competition for the limited functional sites. Moreover, according to the adsorption efficiency for other metal ions, it was not difficult to find that Cd(II) (46.15%) had a relatively higher affinity with dRSM-R, followed by Cu(II) (43.00%), Pb (II) (37.63%), Ni(II) (30.60%) and Zn(II) (28.50%). The most important point is that dRSM-R can adsorb a variety of heavy metal ions at the same time, showing a wider range of applications and practical values for wastewater treatment.

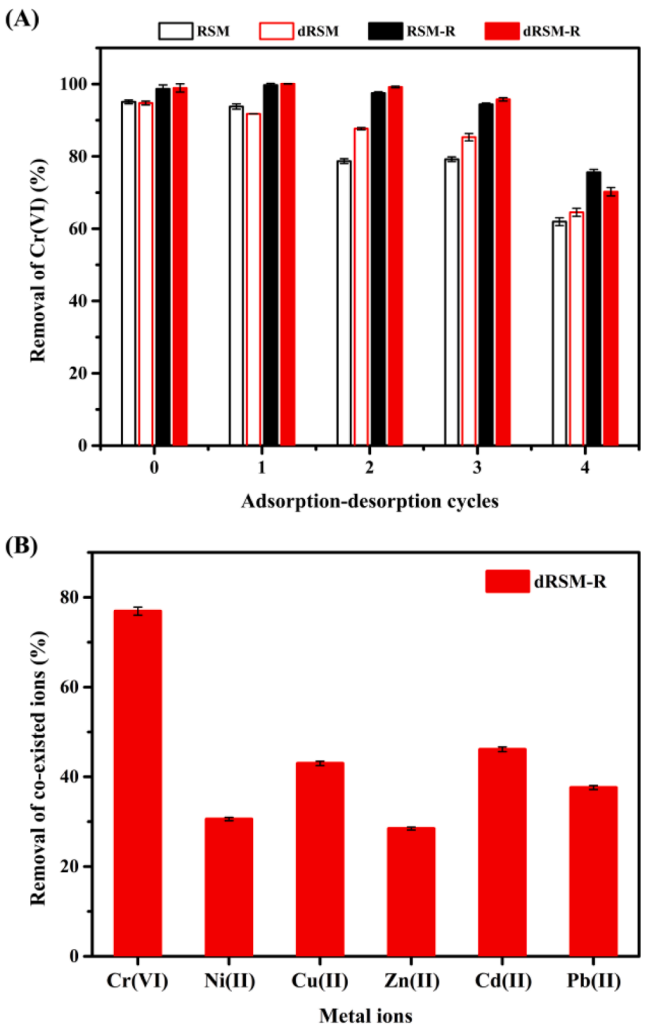


Fig. 5. (A) Regeneration performance of RSM, dRSM, RSM-R and dRSM-R; (B) Adsorption evaluation for co-existed heavy metal ions on dRSM-R.

Table 2
Langmuir and Freundlich adsorption isotherm values for Cr(VI) on RSM and its derivatives.

Sample name	Langmuir model			Freundlich model		
	q_m (mg/g)	k_L (L/mg)	R^2	$1/n$	k_F ((mg•g^{-1})(mg•L^{-1})$^{-n}$)	R^2
RSM	71.45	0.0028	0.9719	0.4672	2.17	0.9974
dRSM	66.53	0.0031	0.9549	0.4455	2.41	0.9858
RSM-R	95.45	0.0026	0.9913	0.4914	2.39	0.9837
dRSM-R	102.09	0.0022	0.9735	0.5234	1.94	0.9826

3.8. Further application and prospect

With the extraction process for agricultural byproducts, most conjugational form phenolics would be converted into free form and separated from residues, which could greatly improve their antioxidant capacities (Alu'datt et al., 2017; Hernández-Jabalera et al., 2015; Zhu

et al., 2018). Moreover, chelation and reduction of heavy metal ions, as well as antimicrobial and free radical scavenging abilities are all related to antioxidant capacities. These improvements extend phenolic extracts' uses in the cosmetic, food, feed and pharmaceutical areas. In this study, we mainly highlighted additional advantages of phenolics with the free form for water treatment as follows (Fig. 6):

(i) Besides Cr(VI), phenolics or phenolic extracts from agricultural byproducts had been proved to be able to chelate various heavy metals in wastewater, such as Ag(I), Ni(II), Cu(II), Zn(II), Cd(II) and Pb(II) (Kuppusamy et al., 2015; Nie et al., 2021). The properties to absorb different ions at the same time and cope with a variety of complex and volatile environmental conditions are the prerequisites for a mature environmental remediation product to occupy the market.

(ii) When the water environment deteriorated, it is usually accompanied by the propagation of harmful microorganisms, which causes further and bigger harm to human health. It has been reported that phenolics extracted from rapeseed byproducts had inhibitory effects on Gram-positive (*Staphylococcus aureus* and *Listeria monocytogenes*) and Gram-negative bacteria (*Escherichia coli*, *Bacillus subtilis*, and *Pseudomonas fluorescens*) (Tymczewska et al., 2021; Wang et al., 2021). Therefore, it will save a lot of costs to kill pathogens by endowing adsorbents with antimicrobial characteristics obtained from phenolic extracts, which has rarely been reported for environmental remediation (Feng et al., 2021).

(iii) The phenolic compounds in rapeseed byproducts were reported to be capable of scavenging free radicals and relieving oxidation of cellular molecules, which is beneficial for human health (Hussain et al., 2019; Kim and Lee, 2017; Li and Guo, 2016; Nandasiri et al., 2019; Pohl et al., 2018; Quinn et al., 2017; Yates et al., 2019). Therefore, when phenolics-treated water was used for human drinks compared with existing ordinary water-filtering media, the ventures of diseases, especially cancer, would be reduced.

Taking all these advantages into consideration, the strategy for RSM biorefining in this study can simultaneously improve the capacities of residue and phenolic extract for heavy metal pollutant remediation with economic management and minimization of wastes. Concomitantly, there are several questions needed to be thoroughly solved. (i) Besides RSM, can the biorefining strategy used in this study be applied to other phenolic-rich agricultural byproducts? In other words, is the pattern of

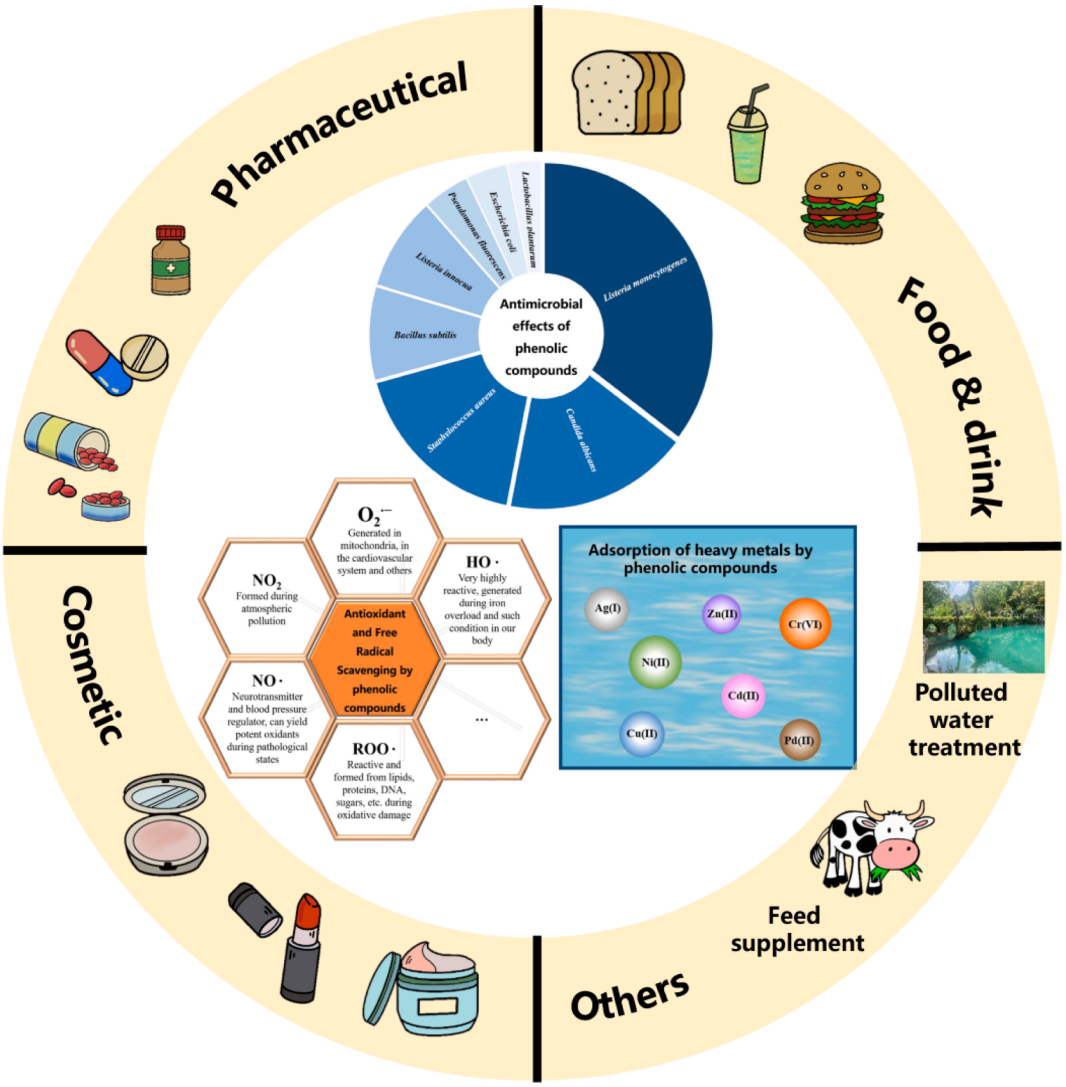


Fig. 6. Additional advantages of phenolics with free form, including metal-chelating (Kuppusamy et al., 2015; Mazurek et al., 2021; Morosanu et al., 2019; Nie et al., 2021), antimicrobial (Engels et al., 2012; Tymczewska et al., 2021; Wang et al., 2021) and free radical scavenging abilities (Pohl et al., 2018; Tymczewska et al., 2021; Yates et al., 2019).

modification through phenolic extraction a universal strategy for improving biosorbents from agricultural byproducts? (ii) How to extensively use residue and phenolic extract, including individual or combined applications? For example, it has been reported that combining biochar with other amendments can significantly reduce heavy metal pollution in soil and further accumulation in plants causing critical health issues in humans and animals (Naeem et al., 2021; Turan, 2019, 2020, 2021, 2022; Zubair et al., 2021). Whether biosorbents modified by phenolic extraction can replace biochar for performing similar functions needs further research. (iii) According to this study, the main mechanism affecting the biosorption capacity of RSM is to change the present state of phenolics therein. This led to another extended thought about whether it is feasible to simplify the process to realize phenolic state change just by pretreatment and then improve the adsorption capacities of agricultural byproducts. In a word, this study provides a solid foundation for the biorefining of agricultural byproducts and biosorbent improvement.

4. Conclusion

This research first exhibits the affirmative aspects of phenolic extraction as a feasible strategy to improve RSM and dRSM's affinity for Cr(VI) by about 21%, and the maximum adsorption capacities on residues could reach about 100 mg/g. The separated phenolic extracts and main component SA therein also demonstrated the ability to eliminate Cr(VI) with positive concentration dependence. Moreover, simulating raw material by remixing 3% separated phenolic extracts or SA with corresponding residues further improved adsorption efficiency by about 12%. All these results revealed that changing the present forms of phenolics could significantly influence agricultural byproducts' function on heavy metal adsorption. In the original agricultural materials, most phenolics existed in a form conjugated with other components, which mutually shielded the Cr(VI) adsorption functional groups of different components. Through extraction process, most phenolics were recovered to the free form, which could release the Cr(VI) adsorption capacity of both phenolics and residues. The adsorption characteristics of residue were explored emphatically by four optimal adsorption parameters, three kinetic models and two isotherms. In addition, advantages of the modified biosorbent derived from RSM with everlasting capacity after 3 adsorption–desorption cycles and excellent abilities for adsorbing multiple co-existed metal ions (Cr(VI), Cd(II), Cu(II), Pb(II), Ni(II) and Zn (II)) under polynary system further proved a wider range of application and practical value for wastewater treatment. In conclusion, this study not only creates a new strategy for modifying biosorbents from agricultural byproducts, but also broadens the applications and managements of RSM means for heavy metal pollutant remediation with zero waste.

CRediT authorship contribution statement

Pei Liu: Investigation, Data curation, Writing – original draft. **Yangmin Gong:** Investigation, Data curation, Formal analysis, Methodology. **Chen Yang:** Investigation, Formal analysis. **Rodrigo Ledesma-Amaro:** Formal analysis, Writing – review & editing. **Young-Kyoung Park:** Formal analysis, Writing – review & editing. **Shiyu Deng:** Investigation. **Yuliang Wang:** Investigation. **Hongbo Wei:** Writing – review & editing. **Wenchao Chen:** Conceptualization, Funding acquisition, Supervision, Writing – review & editing.

Declaration of Competing Interest

The authors declare that they have no known competing financial interests or personal relationships that could have appeared to influence the work reported in this paper.

Data availability

Data will be made available on request.

Acknowledgements

This project is supported by the National Natural Science Foundation of China (Grant Number 32001620), the Natural Science Foundation of Hubei Province (Grant Number 2019CFB378) and the Youth talent development program of Hubei province.

Appendix A. Supplementary data

Supplementary data to this article can be found online at https://doi.org/10.1016/j.wasman.2023.04.024.

References

Alu'datt, M.H., Rababah, T., Alhamad, M.N., Al-Mahasneh, M.A., Almajwal, A., Gammoh, S., Ereifej, K., Johargy, A., Alli, I., 2017. A review of phenolic compounds in oil-bearing plants: distribution, identification and occurrence of phenolic compounds. Food Chem. 218, 99–106. https://doi.org/10.1016/j.foodchem.2016.09.057.

Balasubramanian, U.M., Vaiyazhipalayam Murugaiyan, S., Marimuthu, T., 2020. Enhanced adsorption of Cr(VI), Ni(II) ions from aqueous solution using modified *Eichhornia crassipes* and *Lemna minor*. Environ. Sci. Pollut. Res. 27 (17), 20648–20662. https://doi.org/10.1007/s11356-019-06357-7.

Banerjee, M., Basu, R.K., Das, S.K., 2018. Cr(VI) adsorption by a green adsorbent walnut shell: adsorption studies, regeneration studies, scale-up design and economic feasibility. Process Saf. Environ. Prot. 116, 693–702. https://doi.org/10.1016/j.psep.2018.03.037.

Chen, H., Yang, X., Liu, Y., Lin, X., Wang, J., Zhang, Z., Li, N., Li, Y., Zhang, Y., 2021. KOH modification effectively enhances the Cd and Pb adsorption performance of N-enriched biochar derived from waste chicken feathers. Waste Manage. 130, 82–92. https://doi.org/10.1016/j.wasman.2021.05.015.

Chen, W., Hashimoto, K., Omata, Y., Ohgami, N., Tazaki, A., Deng, Y., Kondo-Ida, L., Intoh, A., Kato, M., 2019. Adsorption of molybdenum by melanin. Environ. Health Prev. Med. 24 (1), 36. https://doi.org/10.1186/s12199-019-0791-y.

Cherdchoo, W., Nithettham, S., Charoenpanich, J., 2019. Removal of Cr(VI) from synthetic wastewater by adsorption onto coffee ground and mixed waste tea. Chemosphere 221, 758–767. https://doi.org/10.1016/j.chemosphere.2019.01.100.

Di Lena, G., Sanchez Del Pulgar, J., Lucarini, M., Durazzo, A., Ondrejickova, P., Oancea, F., Frincu, R.M., Aguzzi, A., Ferrari Nicoli, S., Casini, I., Gabrielli, P., Caproni, R., Cerven, I., Lombardi-Boccia, G., 2021. Valorization potentials of rapeseed meal in a biorefinery perspective: focus on nutritional and bioactive components. Molecules 26 (22), 6787. https://doi.org/10.3390/molecules26226787.

Dong, F., Yan, L., Zhou, X., Huang, S., Liang, J., Zhang, W., Guo, Z., Guo, P., Qian, W., Kong, L., Chu, W., Diao, Z., 2021. Simultaneous adsorption of Cr(VI) and phenol by biochar-based iron oxide composites in water: performance, kinetics and mechanism. J. Hazard. Mater. 416, 125930 https://doi.org/10.1016/j.jhazmat.2021.125930.

Engels, C., Schieber, A., Gänzle, M.G., 2012. Sinapic acid derivatives in defatted Oriental mustard (*Brassica juncea L.*) seed meal extracts using UHPLC-DAD-ESI-MS n and identification of compounds with antibacterial activity. Eur. Food Res. Technol. 234 (3), 535–542. https://doi.org/10.1007/s00217-012-1669-z.

Feng, Y., Wang, H., Xu, J., Du, X., Cheng, X., Du, Z., Wang, H., 2021. Fabrication of MXene/PEI functionalized sodium alginate aerogel and its excellent adsorption behavior for Cr(VI) and Congo Red from aqueous solution. J. Hazard. Mater. 416, 125777 https://doi.org/10.1016/j.jhazmat.2021.125777.

Filipowiak, K., Wieszczycka, K., Buchwald, T., Nowicki, M., Wójcik, G., Aksamitowski, P., Staszak, K., 2021. Reduction-adsorption of chromium(VI) by using IL-imprinted resin -innovative solution for water purification. J. Mol. Liq. 343, 116977 https://doi.org/10.1016/j.molliq.2021.116977.

Halysh, V., Sevastyanova, O., Riazanova, A.V., Pasalskiy, B., Budnyak, T., Lindström, M. E., Kartel, M., 2018. Walnut shells as a potential low-cost lignocellulosic sorbent for dyes and metal ions. Cellulose 25 (8), 4729–4742. https://doi.org/10.1007/s10570-018-1896-y.

He, M., Nian, B., Shi, J., Sun, X., Du, R., Tan, C.P., Xu, Y.J., Liu, Y., 2022. Influence of extraction technology on rapeseed oil functional quality: a study on rapeseed polyphenols. Food Funct. 13 (1), 270–279. https://doi.org/10.1039/d1fo01507a.

Hernández-Jabalera, A., Cortés-Giraldo, I., Dávila-Ortíz, G., Vioque, J., Alaiz, M., Girón-Calle, J., Megías, C., JiménezMartínez, C., 2015. Influence of peptides-phenolics interaction on the antioxidant profile of protein hydrolysates from *Brassica napus*. Food Chem. 178, 346–357. https://doi.org/10.1016/j.foodchem.2014.12.063.

Hu, J., Chen, B., Zhao, J., Zhang, F., Xie, T., Xu, K., Gao, G., Yan, G., Li, H., Li, L., Ji, G., An, H., Li, H., Huang, Q., Zhang, M., Wu, J., Song, W., Zhang, X., Luo, Y., Chris Pires, J., Batley, J., Tian, S., Wu, X., 2022. Genomic selection and genetic architecture of agronomic traits during modern rapeseed breeding. Nat. Genet. 54 (5), 694–704. https://doi.org/10.1038/s41588-022-01055-6.

Hussain, S., Rehman, A.U., Luckett, D.J., Blanchard, C.L., Obied, H.K., Strappe, P., 2019. Phenolic compounds with antioxidant properties from canola meal extracts inhibit adipogenesis. Int. J. Mol. Sci. 21 (1) https://doi.org/10.3390/ijms21010001.
Kekes, T., Kolliopoulos, G., Tzia, C., 2021. Hexavalent chromium adsorption onto crosslinked chitosan and chitosan/β-cyclodextrin beads: novel materials for water decontamination. J. Environ. Chem. Eng. 9 (4), 105581 https://doi.org/10.1016/j.jece.2021.105581.
Kim, Y.S., Lee, J.H., 2017. Effects of hydrolyzed rapeseed cake extract on the quality characteristics of mayonnaise dressing. J. Food Sci. 82 (12), 2847–2856. https://doi.org/10.1111/1750-3841.13979.
Kuppusamy, S., Thavamani, P., Megharaj, M., Naidu, R., 2015. Bioremediation potential of natural polyphenol rich green wastes: a review of current research and recommendations for future directions. Environ. Technol. Inno. 4, 17–28. https://doi.org/10.1016/j.eti.2015.04.001.
Le Bourvellec, C., Renard, C.M.G.C., 2010. Interactions between polyphenols and macromolecules: quantification methods and mechanisms. Crit. Rev. Food Sci. Nutr. 52, 213–248. https://doi.org/10.1080/10408398.2010.499808.
Leng, L., Xu, S., Liu, R., Yu, T., Zhuo, X., Leng, S., Xiong, Q., Huang, H., 2020. Nitrogen containing functional groups of biochar: an overview. Bioresour. Technol. 298, 122286 https://doi.org/10.1016/j.biortech.2019.122286.
Li, J., Guo, Z., 2016. Concurrent extraction and transformation of bioactive phenolic compounds from rapeseed meal using pressurized solvent extraction system. Ind. Crops Prod. 94, 152–159. https://doi.org/10.1016/j.indcrop.2016.08.045.
Li, Y., He, D., Li, B., Lund, M.N., Xing, Y., Wang, Y., Li, F., Cao, X., Liu, Y., Chen, X., Yu, J., Zhu, J., Zhang, M., Wang, Q., Zhang, Y., Li, B., Wang, J., Xing, X., Li, L., 2021. Engineering polyphenols with biological functions via polyphenol-protein interactions as additives for functional foods. Trends Food Sci. Technol. 110, 470–482. https://doi.org/10.1016/j.tifs.2021.02.009.
Mallik, A.K., Moktadir, M.A., Rahman, M.A., Shahruzzaman, M., Rahman, M.M., 2022. Progress in surface-modified silicas for Cr(VI) adsorption: a review. J. Hazard. Mater. 423, 127041 https://doi.org/10.1016/j.jhazmat.2021.127041.
Mazurek, K., Druzynski, S., Kielkowska, U., Szlyk, E., 2021. New separation material obtained from waste rapeseed cake for copper(II) and zinc(II) removal from the industrial wastewater. Materials 14 (10), 2566. https://doi.org/10.3390/ma14102566.
Morosanu, I., Teodosiu, C., Coroaba, A., Paduraru, C., 2019. Sequencing batch biosorption of micropollutants from aqueous effluents by rapeseed waste: experimental assessment and statistical modelling. J. Environ. Manage. 230, 110–118. https://doi.org/10.1016/j.jenvman.2018.09.075.
Naeem, I., Masood, N., Turan, V., Iqbal, M., 2021. Prospective usage of magnesium potassium phosphate cement combined with *Bougainvillea alba* derived biochar to reduce Pb bioavailability in soil and its uptake by *Spinacia oleracea* L. Ecotoxicol. Environ. Saf. 208, 111723 https://doi.org/10.1016/j.ecoenv.2020.111723.
Nahar, K., Chowdhury, M.A.K., Chowdhury, M.A.H., Rahman, A., Mohiuddin, K.M., 2018. Heavy metals in handloom-dyeing effluents and their biosorption by agricultural byproducts. Environ. Sci. Pollut. Res. 25 (8), 7954–7967. https://doi.org/10.1007/s11356-017-1166-9.
Nandasiri, R., Eskin, N.A.M., Thiyam-Hollander, U., 2019. Antioxidative Polyphenols of Canola Meal Extracted by High Pressure: Impact of Temperature and Solvents. J. Food Sci. 84 (11), 3117–3128. https://doi.org/10.1111/1750-3841.14799.
Nie, L., Chang, P., Liang, S., Hu, K., Hua, D., Liu, S., Sun, J., Sun, M., Wang, T., Okoro, O. V., Shavandi, A., 2021. Polyphenol rich green tea waste hydrogel for removal of copper and chromium ions from aqueous solution. Clean. Eng. Technol. 4, 100167 https://doi.org/10.1016/j.clet.2021.100167.
Orooji, Y., Nezafat, Z., Nasrollahzadeh, M., Kamali, T.A., 2021. Polysaccharide-based (nano)materials for Cr(VI) removal. Int J Biol Macromol. 188, 950–973. https://doi.org/10.1016/j.ijbiomac.2021.07.182.
Pohl, F., Goua, M., Bermano, G., Russell, W.R., Scobbie, L., Maciel, P., Kong Thoo Lin, P., 2018. Revalorisation of rapeseed pomace extracts: an in vitro study into its antioxidant and DNA protective properties. Food Chem. 239, 323–332. https://doi.org/10.1016/j.foodchem.2017.06.129.
Qiu, Y., Zhang, Q., Gao, B., Li, M., Fan, Z., Sang, W., Hao, H., Wei, X., 2020. Removal mechanisms of Cr(VI) and Cr(III) by biochar supported nanosized zero-valent iron: synergy of adsorption, reduction and transformation. Environ. Pollut. 265, 115018 https://doi.org/10.1016/j.envpol.2020.115018.
Quinn, L., Gray, S.G., Meaney, S., Finn, S., McLoughlin, P., Hayes, M., 2017. Extraction and quantification of sinapinic acid from Irish rapeseed meal and assessment of angiotensin-I converting enzyme (ACE-I) inhibitory activity. J. Agric. Food. Chem. 65 (32), 6886–6892. https://doi.org/10.1021/acs.jafc.7b02670.
Quíros-Sauceda, A.E., Palafox-Carlos, H., Śayago-Ayerdi, S.G., Ayala-Zavala, J.F., Bello-Perez, L.A.,·Alvarez-Parrilla, E., de la Rosa, L.A., Gonźalez-Córdova, A.F., Gonźalez-Aguilar, G.A., 2014. Dietary fiber and phenolic compounds as functional ingredients: interaction and possible effect after ingestion. Food Funct. 5(6), 1063–1072. 10.1039/c4fo00073k.
Quyen, V.T., Pham, T.H., Kim, J., Thanh, D.M., Thang, P.Q., Van Le, Q., Jung, S.H., Kim, T., 2021. Biosorbent derived from coffee husk for efficient removal of toxic heavy metals from wastewater. Chemosphere 284, 131312. https://doi.org/10.1016/j.chemosphere.2021.131312.
Rasool, B., Mahmood ur, R., Zubair, M., Khan, M.A., Ramzani, P.M.A., Dradrach, A., Turan, V., Iqbal, M., Khan, S.A., Tauqeer, H.M., Farhad, M., Virk, Z.A., Iqbal, M., 2022. Synergetic Efficacy of amending Pb-polluted soil with P-loaded jujube (*Ziziphus mauritiana*) twigs biochar and foliar chitosan application for reducing Pb distribution in moringa leaf extract and improving its anti-cancer potential. Water Air Soil Pollut. 233(8). 10.1007/s11270-022-05807-2.
Ravindran, R., Jaiswal, A.K., 2016. A comprehensive review on pre-treatment strategy for lignocellulosic food industry waste: challenges and opportunities. Bioresour. Technol. 199, 92–102. https://doi.org/10.1016/j.biortech.2015.07.106.
Shan, R., Shi, Y., Gu, J., Bi, J., Yuan, H., Luo, B., Chen, Y., 2020. Aqueous Cr(VI) removal by biochar derived from waste mangosteen shells: role of pyrolysis and modification on its absorption process. J. Environ. Chem. Eng. 8 (4), 103885 https://doi.org/10.1016/j.jece.2020.103885.
Shi, X., Qiao, Y., An, X., Tian, Y., Zhou, H., 2020. High-capacity adsorption of Cr(VI) by lignin-based composite: characterization, performance and mechanism. Int. J. Biol. Macromol. 159, 839–849. https://doi.org/10.1016/j.ijbiomac.2020.05.130.
Suksabye, P., Thiravetyan, P., 2012. Cr(VI) adsorption from electroplating plating wastewater by chemically modified coir pith. J. Environ. Manage. 102, 1–8. https://doi.org/10.1016/j.jenvman.2011.10.020.
Swarnalatha, K., Ayoob, S., 2016. Adsorption studies on coir pith for heavy metal removal. Int. J. Sustain. Eng. 9 (4), 259–265. https://doi.org/10.1080/19397038.2016.1152323.
Tauqeer, H.M., Basharat, Z., Adnan Ramzani, P.M., Farhad, M., Lewinska, K., Turan, V., Karczewska, A., Khan, S.A., Faran, G.E., Iqbal, M., 2022. *Aspergillus niger*-mediated release of phosphates from fish bone char reduces Pb phytoavailability in Pb-acid batteries polluted soil, and accumulation in fenugreek. Environ. Pollut. 313, 120064 https://doi.org/10.1016/j.envpol.2022.120064.
Thakur, M., Nanda, V., 2019. Process optimization of polyphenol-rich milk powder using bee pollen based on physicochemical and functional properties. J. Food Process Eng. 42 (6) https://doi.org/10.1111/jfpe.13148.
Turan, V., Khan, S.A., Mahmood Ur, R., Iqbal, M., Ramzani, P.M.A., Fatima, M., 2018a. Promoting the productivity and quality of brinjal aligned with heavy metals immobilization in a wastewater irrigated heavy metal polluted soil with biochar and chitosan. Ecotoxicol. Environ. Saf. 161, 409–419. https://doi.org/10.1016/j.ecoenv.2018.05.082.
Turan, V., Ramzani, P.M.A., Ali, Q., Abbas, F., Iqbal, M., Irum, A., Khan, W.U.D., 2018b. Alleviation of nickel toxicity and an improvement in zinc bioavailability in sunflower seed with chitosan and biochar application in pH adjusted nickel contaminated soil. Arch. Agron. Soil Sci. 64 (8), 1053–1067. https://doi.org/10.1080/03650340.2017.1410542.
Turan, V., 2019. Confident performance of chitosan and pistachio shell biochar on reducing Ni bioavailability in soil and plant plus improved the soil enzymatic activities, antioxidant defense system and nutritional quality of lettuce. Ecotoxicol. Environ. Saf. 183, 109594 https://doi.org/10.1016/j.ecoenv.2019.109594.
Turan, V., 2020. Potential of pistachio shell biochar and dicalcium phosphate combination to reduce Pb speciation in spinach, improved soil enzymatic activities, plant nutritional quality, and antioxidant defense system. Chemosphere 245, 125611. https://doi.org/10.1016/j.chemosphere.2019.125611.
Turan, V., 2021. *Arbuscular mycorrhizal* fungi and pistachio husk biochar combination reduces Ni distribution in mungbean plant and improves plant antioxidants and soil enzymes. Physiol. Plant 173 (1), 418–429. https://doi.org/10.1111/ppl.13490.
Turan, V., 2022. Calcite in combination with olive pulp biochar reduces Ni mobility in soil and its distribution in chili plant. Int. J. Phytorem. 24 (2), 166–176. https://doi.org/10.1080/15226514.2021.1929826.
Tymczewska, A., Furtado, B.U., Nowaczyk, J., Hrynkiewicz, K., Szydlowska-Czerniak, A., 2021. Development and characterization of active gelatin films loaded with rapeseed meal extracts. Materials 14 (11), 2869. https://doi.org/10.3390/ma14112869.
Vázquez, G., Calvo, M., Freire, M.S., González-Alvarez, J., Antorrena, G., 2009. Chestnut shell as heavy metal adsorbent: optimization study of lead, copper and zinc cations removal. J. Hazard. Mater. 172, 1402–1414. https://doi.org/10.1016/j.jhazmat.2009.08.006.
Wang, M., Yang, C., François, J.M., Wan, X., Deng, Q., Feng, D., Deng, S., Chen, S., Huang, F., Chen, W., Gong, Y., 2021. A two-step strategy for high-value-added utilization of rapeseed meal by concurrent improvement of phenolic extraction and protein conversion for microbial iturin A production. Front. Bioeng. Biotech. 975 https://doi.org/10.3389/fbioe.2021.735714.
Yang, J., Roozalipour, S.P.L., Berton-Carabin, C.C., Nikiforidis, C.V., Linden, E.v.d., Sagis, L.M.C., 2021. Air-water interfacial and foaming properties of whey protein - sinapic acid mixtures. Food Hydrocolloids 112, 106467. 10.1016/j.foodhyd.2020.106467.
Yates, K., Pohl, F., Busch, M., Mozer, A., Watters, L., Shiryaev, A., Kong Thoo Lin, P., 2019. Determination of sinapine in rapeseed pomace extract: its antioxidant and acetylcholinesterase inhibition properties. Food Chem. 276, 768–775. https://doi.org/10.1016/j.foodchem.2018.10.045.
Zhang, T., Hu, L., Zhang, M., Jiang, M., Fiedler, H., Bai, W., Wang, X., Zhang, D., Li, Z., 2019. Cr(VI) removal from soils and groundwater using an integrated adsorption and microbial fuel cell (A-MFC) technology. Environ. Pollut. 252, 1399–1405. https://doi.org/10.1016/j.envpol.2019.06.051.
Zhang, X., Fu, W., Yin, Y., Chen, Z., Qiu, R., Simonnot, M., Wang, X., 2018. Adsorption-reduction removal of Cr(VI) by tobacco petiole pyrolytic biochar: batch experiment, kinetic and mechanism studies. Bioresour. Technol. 268, 149–157. https://doi.org/10.1016/j.biortech.2018.07.125.
Zhao, N., Zhao, C., Tsang, D.C.W., Liu, K., Zhu, L., Zhang, W., Zhang, J., Tang, Y., Qiu, R., 2021. Microscopic mechanism about the selective adsorption of Cr(VI) from salt solution on O-rich and N-rich biochars. J. Hazard. Mater. 404, 124162 https://doi.org/10.1016/j.jhazmat.2020.124162.
Zhu, J., Zhang, D., Tang, H., Zhao, G., 2018. Structure relationship of non-covalent interactions between phenolic acids and arabinan-rich pectic polysaccharides from rapeseed meal. Int. J. Biol. Macromol. 120, 2597–2603. https://doi.org/10.1016/j.ijbiomac.2018.09.036.
Zubair, M., Ramzani, P.M.A., Rasool, B., Khan, M.A., Akhtar, I., Turan, V., Tauqeer, H.M., Farhad, M., Khan, S.A., Iqbal, J., Iqbal, M., 2021. Efficacy of chitosan-coated textile

waste biochar applied to Cd-polluted soil for reducing Cd mobility in soil and its distribution in moringa (*Moringa oleifera L.*). J. Environ. Manage. 284, 112047 https://doi.org/10.1016/j.jenvman.2021.112047.